Asymmetric paramagnetic bimetallocenes of nickel and cobalt†‡

Harald Hilbig and Frank H. Köhler*

Anorganisch-chemisches Institut, Technische Universität München, D-85747 Garching, Germany. E-mail: f.h.koehler@lrz.tu-muenchen.de

Received (in Strasbourg, France) 5th April 2001, Accepted 8th June 2001
First published as an Advance Article on the web 21st August 2001

Reaction of tetramethylpentafulvalene dianion (**2**) with $(C_5Me_5)Ni(acac)$ (acac = acetylacetonate) gave the asymmetric tetradecamethylbinickelocene Ni′Ni″ (M′ and M″ = penta- and nonamethylmetallocenyl, respectively). When $(C_5Me_5)Co(acac)$ was used in the reaction, Co′-C_5Me_4, a tetramethylpentafulvalene stabilized by a $(C_5Me_5)Co$ fragment, was obtained. The same reaction, followed immediately by oxidation with one equivalent of $[Cp_2Fe]^+[PF_6]^-$ and two equivalents of $AgNO_3$, gave the tetradecamethylbicobaltocenium mono- and dications, Co′Co″$^+$ and Co′$^+$Co″$^+$, respectively. Two different metals were introduced in a tetradecamethylbimetallocene by first synthesizing a pentamethylnickelocene, which was coupled to a tetramethylcyclopentadiene (Ni′-C_5Me_4H). When this was deprotonated, the expected anion Ni′-$[C_5Me_4]^-$ rearranged to Ni″-$[C_5H_4]^-$. MO calculations demonstrate that the rearrangement occurs through the shift of a $[(C_5Me_5)Ni]^+$ fragment from the non-methylated to the tetramethylated part of **2**. Reaction of Ni″-$[C_5H_4]^-$ with $(C_5Me_5)Co(acac)$ gave the mixed-metal compound Co′Ni″.

Ni′Ni″ and Co′Ni″ have four and three unpaired electrons, respectively. They are shown by temperature-dependent ^1H NMR spectra to couple antiferromagnetically; data fits yield $J = -195$ and -174 cm^{-1}, respectively. All paramagnetic compounds gave strongly shifted ^1H and ^{13}C NMR signals. The experimental shifts were converted to contact shifts that reflect the spin distribution within the molecules. The spin density proved to be delocalized from a given paramagnetic metallocene to the adjacent metallocene, regardless of whether it was diamagnetic or paramagnetic. In the latter case this led to antiferromagnetic coupling. The spin distribution was analyzed by means of MO calculations.

Cyclic voltammetry shows Co′$^+$Co″$^+$, Ni′Ni″ and Co′Ni″ to undergo electron transfers that introduce up to one negative and four positive charges. The redox potentials proved to depend mainly on methylation and charge localization.

Interacting unpaired electrons in a solid material give rise to interesting magnetic behavior including spontaneous magnetization, which is a precondition for their use as, for example, permanent magnets. The magnetically active centers are often transition metal ions that are interconnected by means of ligand bridging.[1] This approach can also be viewed as the (preferably rational) assembly of paramagnetic building blocks; hence the widely accepted term "molecule-based magnetic materials". The most successful attempts are based on coordination compounds while the use of exclusively organometallic building blocks is much less advanced.

In this context the present work focuses on paramagnetic metallocenes. When interconnected by silyl groups as in **A**, they show weak antiferromagnetic interactions regardless of the nature of the engaged metals.[2] By way of contrast, the magnetism of directly coupled metallocenes, more precisely the decamethylbimetallocenes **B**[3a–c] and their cations,[3d,e] varies strongly: coupling of two vanadocenes (or chromocenes), nickelocenes, and cobaltocenes leads to weak antiferromagnetic, strong antiferromagnetic, and strong ferromagnetic interactions, respectively. Related compounds are **C** and **D**, where conjugated bridging is realized by *s*-indacene and *as*-indacene ligands.[4] Here again the magnetic moments not only point to antiferromagnetic but also to ferromagnetic interactions. Of course, one would like to adjust the magnetic behavior of these linked metallocenes, but guidelines are not known so far except for **A**.[2a] An important criterion for understanding the interaction between all sorts of potential building blocks of magnetic materials is the distribution of unpaired electron spin (abbreviated as spin or spin density throughout this paper), and much effort has been devoted to the determination of spin densities.[5]

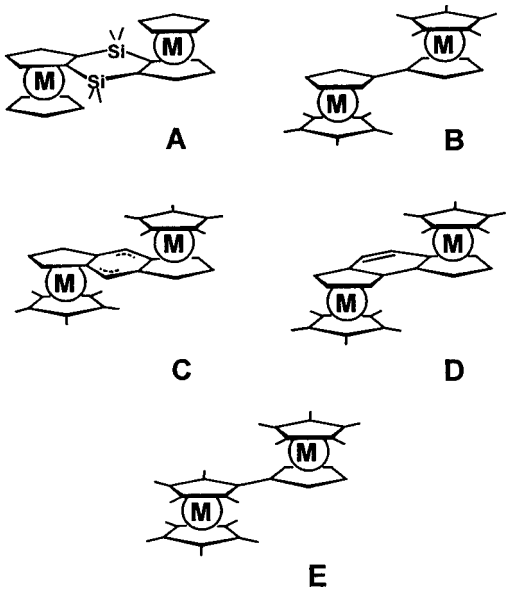

Therefore, the aim of the present work was to synthesize paramagnetic bimetallocenes that would have spin distributions different from those known for the parent compounds

† *In memoriam* Professor Olivier Kahn.
‡ Electronic supplementary information (ESI) available: Fig. SI 1–4. See http://www.rsc.org/suppdata/nj/b1/b103122h/

 DOI: 10.1039/b103122h

B.[3] An extreme change of the spin distribution would be localization of the unpaired electrons in one half of a bimetallocene. One may think of realizing this goal by oxidation of the neutral symmetric bimetallocenes to mixed-valence derivatives. However, it turns out that the valencies of these species oscillate with high rates.[3d,e,6] To overcome this problem we have decided to lower the symmetry of the bridging fulvalene ligand of **B** by methylating one half so that bimetallocenes of type **E** would result. This approach would also allow us to introduce different metals in a bimetallocene. This was another aim of our study as it was not known how different paramagnetic centers would contribute to the overall distribution of the spin in this type of molecule. In previous work we have found that all isomers of the hydrocarbon precursor 1,2,3,4-tetramethydihydrofulvalene (**1**) can be deprotonated to give not only the dianion (**2**)[7a] but also the monoanion (**3**).[7b] As will be shown below, this is mandatory for attaching transition metal fragments step-by-step. We have selected cobaltocene- and nickelocene-derived model compounds to test the synthetic approach and to study the properties of asymmetric bimetallocenes by placing emphasis on NMR spectroscopy and cyclic voltammetry.

Results

Synthesis

The synthesis of homometallic asymmetric bimetallocenes (see Scheme 1) started by doubly deprotonating **1** and its isomers with *t*-butyllithium.[7a] Reaction of the resulting dianion (**2**) with $(C_5Me_5)Ni(acac)$[8] (acac = acetylacetonate) gave tetradecamethylnickelocene (Ni′Ni″) in 86% yield (here Ni′ and Ni″ stand for the penta- and nonamethylated nickelocene halves, respectively; the abbreviation pattern is also applied for other bimetallocenes and precursors thereof). Even in dilute solution Ni′Ni″ is dark violet in contrast to mostly light green mononuclear nickelocenes. Actually, the electronic spectrum of Ni′Ni″ (Fig. SI 1) resembles that of decamethylbinickelocene (Ni′Ni′),[3c] that is, it has intense features above 500 nm that are responsible for the deep color. While the bands at 540 (Ni′Ni″) and 528 nm (Ni′Ni′) are very similar, the second band of Ni′Ni″ near 600 nm is much stronger than the corresponding weak shoulder of Ni′Ni′. We have previously related the color difference of nickelocene and binickelocene to magnetic exchange and simultaneous excitation of neighboring nickel centers.[3c,9]

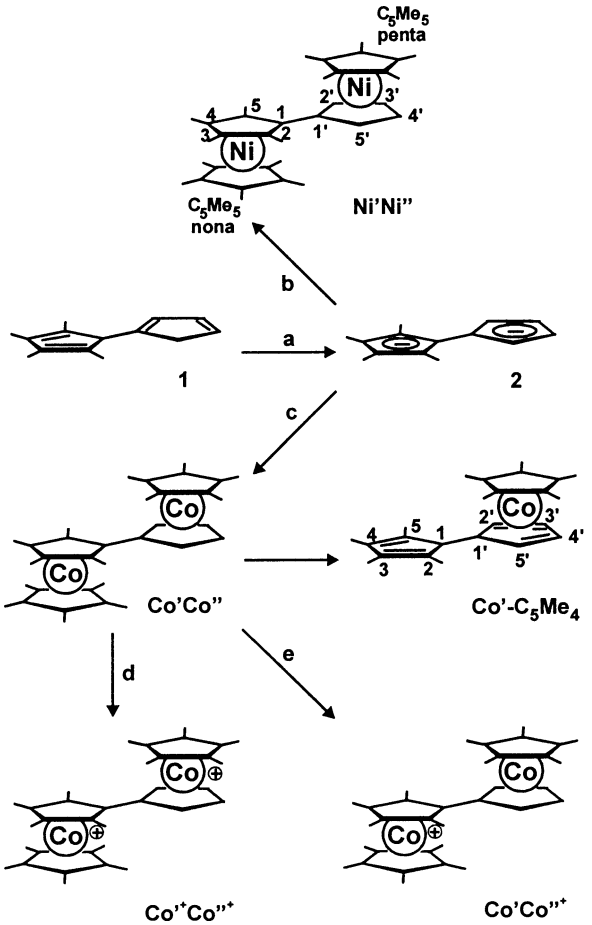

Scheme 1 Synthesis of homometallic tetradecamethylbimetallocenes. (a) *t*-BuLi; (b) $(C_5Me_5)Ni(acac)$; (c) $(C_5Me_5)Co(acac)$; (d) $AgNO_3$; (e) $[Cp_2Fe]^+[PF_6]^-$.

The compound Ni′Ni″ is air-sensitive and very readily soluble in solvents that do not react (aliphatic and aromatic hydrocarbons, ethers, acetone). This made purification tedious, and in the elemental analysis we could not avoid some divergence from the expected nickel content. On the other hand, ^1H NMR spectroscopy (see Fig. 1 below) showed that diamagnetic and paramagnetic impurities were negligible. Similar difficulties were encountered with other compounds of this type.

Reaction of dianion **2** with two equivalents of $(C_5Me_5)Co(acac)$[8] at −78 °C and subsequent warming to ambient temperature gave a dark blue product while the target bicobaltocene (Co′Co″) was expected to be brown.[3c] The ^1H NMR spectrum of the reaction mixture showed intense signals in the range of diamagnetic compounds and those of $(C_5Me_5)Co(acac)$ [$\delta(^1H)$/signal half width in Hz: 52.0/4800 (15H, C_5Me_5), −14.1/770 (6H, CH_3 of acac), −23.9/1230 (1H, CH of acac), in toluene-d_8]. Retrospect comparison of the signal areas of the blue product and of $(C_5Me_5)Co(acac)$ revealed that only one equivalent of $(C_5Me_5)Co(acac)$ had reacted. Based on mass and NMR spectroscopies the blue compound was identified as tetramethylpentafulvalene stabilized by a $(C_5Me_5)Co$ fragment (Co′-C_5Me_4). After separation of $(C_5Me_5)Co(acac)$ the ^1H NMR spectrum showed an AA′BB′ pattern centered at 4.32 ppm that is expected for an η^4-coordinated fulvalene moiety; the signal shift range is known from $(C_5R_5)Co(diene)$.[10] The remaining three signals belong to the methyl groups of C_5Me_5 and the tetramethylated half of the pentafulvalene ligand. The compound Co′-C_5Me_4 is very soluble in hexane and ether and very sensitive to air; its mode of formation is unclear.

When the reaction between **2** and $(C_5Me_5)Co(acac)$ was carried out at ambient temperature a brown mixture was obtained. We were unable to isolate the expected compound Co′Co″ from this mixture. Therefore, in a second run, the brown mixture was oxidized with excess $AgNO_3$. After work-up yellow tetradecamethylbicobaltocenium dication ($Co'^+Co''^+$) was isolated as the hexafluorophosphate in 86% yield. The corresponding monocation ($Co'Co''^+$) was obtained in 74% yield as the salt $[Co'Co''^+][PF_6]^-$ by oxidizing the brown mixture with slightly less than one equivalent of $[Cp_2Fe]^+[PF_6]^-$. Unlike $[Co'^+Co''^+][PF_6]^-_2$ the green mixed-valence compound $[Co'Co''^+][PF_6]^-$ is air-sensitive.

The approach to paramagnetic mixed-metal bimetallocenes was realized with nickel and cobalt (Scheme 2). Thus, reaction of monoanion **3** with $(C_5Me_5)Ni(acac)$ gave the green mixed-ligand nickelocene Ni′-C_5Me_4H, which was deprotonated with NaH. We were unable to find reaction conditions that allowed us to observe the expected anion Ni′-$[C_5Me_4]^-$. Instead the rearranged anion Ni″-$[C_5H_4]^-$ was obtained as the sodium salt in about 80% yield. Further reaction of Ni″-$[C_5H_4]$Na with $(C_5Me_5)Co(acac)$ gave the mixed-metal tetradecamethylbimetallocene Co′Ni″ in modest yield. The neutral compounds Ni′-C_5Me_4H and Co′Ni″ are very soluble in hexane, toluene, and ethers, while Ni″-$[C_5H_4]$Na readily dissolves in non-oxidizing polar solvents such as DMSO and THF. All compounds decompose in the presence of oxygen,

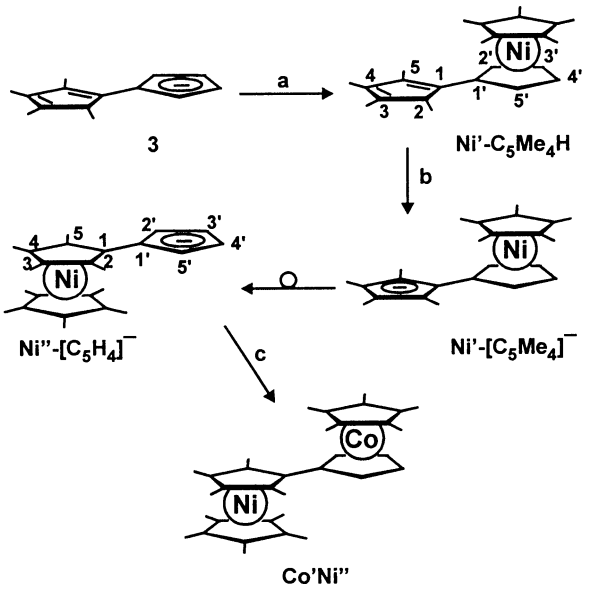

Scheme 2 Synthesis of the heterometallic tetradecamethylbimetallocene Co′Ni″. (a) (C_5Me_5)Ni(acac); (b) NaH; (c) (C_5Me_5)Co(acac).

Ni″-$[C_5H_4]$Na and Co′Ni″ are also moisture-sensitive. The characterization of these compounds is part of the following section.

NMR results for paramagnetic compounds

The ^{1}H and ^{13}C NMR spectra of Ni′Ni″ resemble those of Ni′Ni′.[3b,c] Owing to the lower symmetry, Ni′Ni″ yields two proton signals for the (C_5Me_5) ligands (Fig. 1), and two additional methyl proton signals are seen for the pentafulvalene bridge. In the ^{13}C NMR spectrum of Ni′Ni″ (Fig. SI 2) the two expected signals of (C_5Me_5) and those of $C_{2/5}$ and $C_{2'/5'}$ virtually coincide while they are resolved in the case of (C_5Me_5), $C_{3/4}$ and $C_{3'/4'}$ and C_1 and $C_{1'}$. The signals of the methyl groups at $C_{2/5}$ and $C_{3/4}$ appear close to those of (C_5Me_5), as expected. The more detailed signal assignment follows from comparison with Ni″-$[C_5H_4]^-$ and Co′Co″$^+$ (see Discussion).

Temperature-dependent proton NMR studies (Fig. 1) reveal the presence of a very small amount of an unknown impurity whose signal shifts increased on lowering the temperature as expected from the Curie law. By contrast, the temperature dependence of all signals of Ni′Ni″ deviate in a way that is characteristic of antiferromagnetic interaction.

The mixed-valence bicobaltocenium cation Co′Co″$^+$ features separate sets of signals for its two halves in both the ^{1}H and ^{13}C NMR spectra (Fig. 2). As shown below by cyclic voltammetry, the charge of Co′Co″$^+$ is localized on the cobalt atom of the nonamethylated half, and hence the unpaired electron must be located mainly on the cobalt atom of the pentamethylated half. The NMR signals of the latter fragment were distinguishable from the others because they had larger shifts and widths. In addition, many signals or groups of signals were identified by their areas. For some of the ^{13}C NMR signals the multiplet pattern due to the one-bond C,H coupling could be resolved. Further signal assignment was based on MO calculations, which showed that the signals of $C_{1'}$ should be shifted strongly to high frequency. Since no separate signal could be detected in this range, we assume that it is hidden under the broad signal at 340 ppm. The NMR signals of Co′Co″$^+$ were distinguished easily from those of a diamagnetic impurity, because most of them were more shifted and because all moved when the temperature was changed.

The nickelocenes Ni′-C_5Me_4H and Ni″-$[C_5H_4]$Na, which are substituted by cyclopentadiene and cyclopentadienyl, respectively, gave a surprising ^{1}H NMR result (Fig. 3). As expected for nickelocenes, Ni′-C_5Me_4H shows large negative shifts for the ring proton signals and the signal of (C_5Me_5) near 240 ppm. After deprotonation of the cyclopentadiene moiety the signals near −205 ppm disappear, and two new ones are seen above 240 ppm. This proves that the pentafulvalene ligand is bonded to nickel with its tetramethylated half and that, therefore, a rearrangement must have occurred on passing from Ni′-C_5Me_4H (*via* Ni′-$[C_5Me_4]^-$) to Ni″-$[C_5H_4]^-$. Accordingly, the two signals of $H_{2'/5'}$ and $H_{3'/4'}$

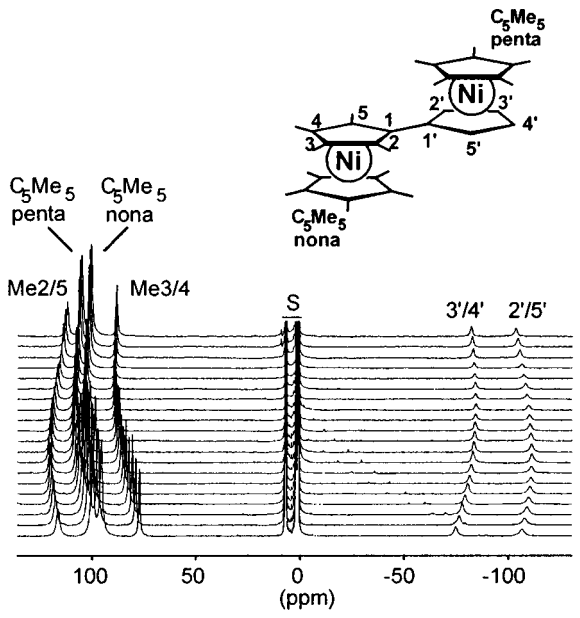

Fig. 1 Temperature dependence of the ^{1}H NMR spectrum of Ni′Ni″ dissolved in toluene-d_8. The temperature runs from 183 (lowest trace) to 385 K. S = solvent.

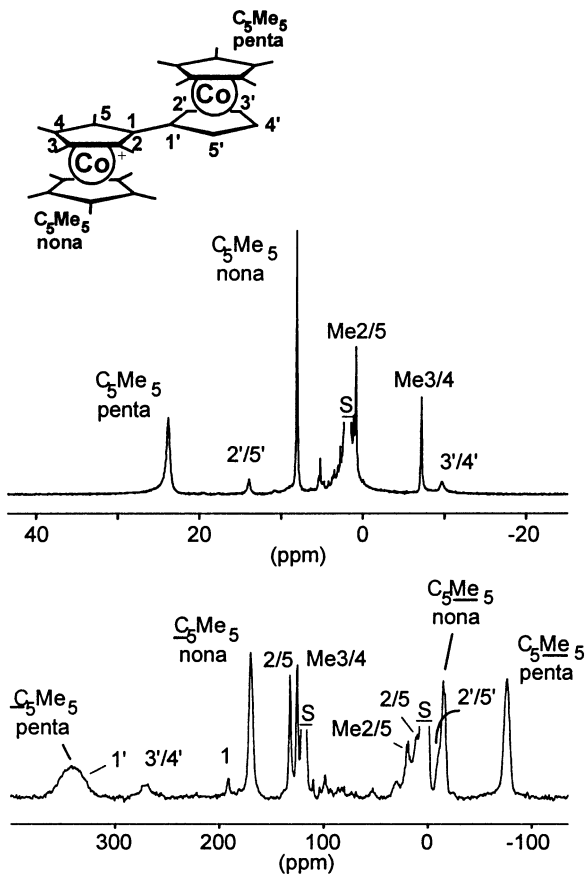

Fig. 2 NMR spectra of $[Co'Co''^+][PF_6]^-$ dissolved in CD_3CN. Top: ^{1}H NMR at 300 K; bottom: ^{13}C NMR at 343 K. S = solvent.

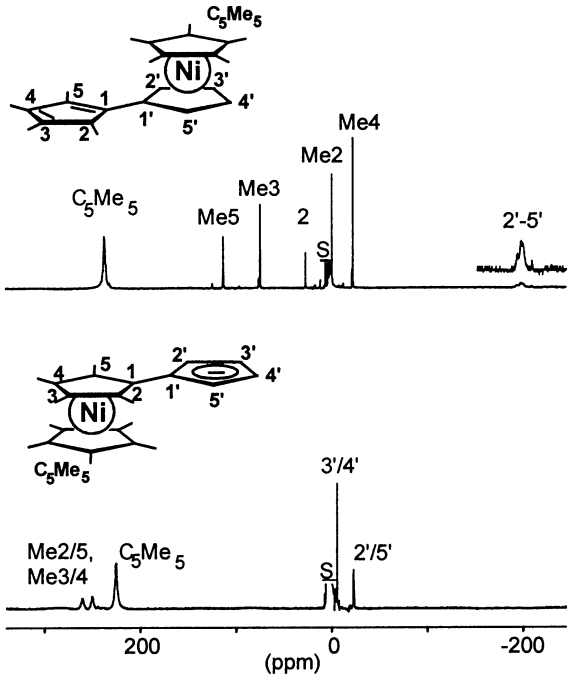

Fig. 3 ^{1}H NMR spectra of nickelocene derivatives at 298 K. Top: Ni′-C_5Me_4H in THF-d_8, bottom: Ni″-$[C_5H_4]$Na in DMSO-d_6. S = solvent.

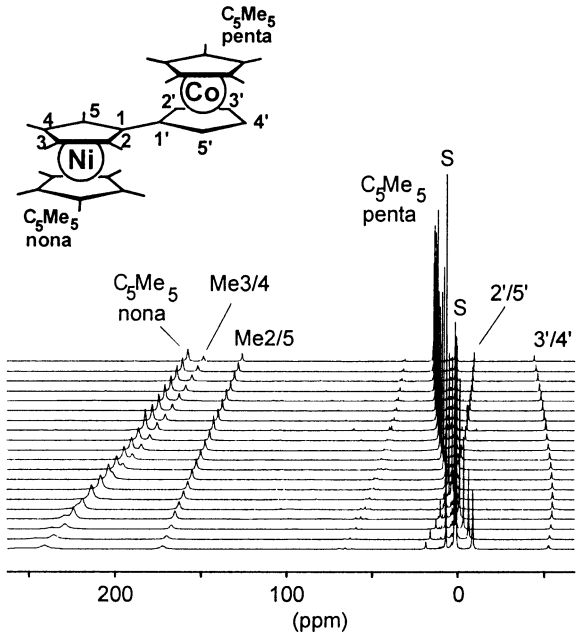

Fig. 4 Temperature dependence of the ^{1}H NMR spectrum of Co′Ni″ dissolved in toluene-d_8. The temperature runs from 171 (lowest brace) to 375 K. S = solvent.

moved from −205 ppm to about −15 ppm while the signal of (C_5Me_5) did not change very much. Again assignment details of the methyl and ring protons of Ni′-C_5Me_4H and Ni″-$[C_5H_4]^-$ were derived from MO calculations.

The rearrangement was confirmed by the ^{13}C NMR spectra of Ni′-C_5Me_4H and Ni″-$[C_5H_4]$Na (Fig. SI 3). For instance, the Me_{2-5} signals of Ni′-C_5Me_4H, which appear between 220 and −220 ppm, are shifted to about −660 ppm after deprotonation to Ni″-$[C_5H_4]$Na. A very similar compound is $(C_5Me_4H)_2Ni$, whose methyl carbon signals have been found near −650 ppm.[11] The ring carbon signals of nickelocenes are strongly shifted (>1000 ppm) and very broad (>3200 Hz).[11,12] In the case of Ni′-C_5Me_4H and Ni″-$[C_5H_4]$Na signals were found in this range, but they were partly overlapped and the signal-to-noise ratio was not sufficient for a reliable analysis. Inspection of the spectra of Ni′-C_5Me_4H (Fig. 3 and SI 3) reveals a second set of much less intense paramagnetically shifted signals. We ascribe this set to the second diastereomer resulting from the asymmetric carbon C_4 and planar chirality of Ni′-C_5Me_4H by analogy to the corresponding ferrocene.[7b] Another conceivable isomer, which has the methylene carbon in position 3 rather than 2, has been excluded for the ferrocene, and the same is assumed for Ni′-C_5Me_4H.

The ^{1}H NMR spectrum of the mixed-metal bimetallocene Co′Ni″ (Fig. 4) is simple. It shows a methyl signal pattern for the nonamethylnickelocene half around 200 ppm similar to that of Ni″-$[C_5H_4]$Na, while the areas of the remaining paramagnetically shifted signals establish the pentamethylcobaltocene half. In the ^{13}C NMR spectrum of Co′Ni″ (Fig. SI 4) the ring carbon signals of the nickelocene half appear between 1000 and 1200 ppm and those of the (C_5Me_5)Co fragment near 280 ppm. All methyl carbon signals have negative shifts, which reflects the well-known change of the spin sign on passing from the ring carbon atoms to adjacent atoms. Again, the signals of the nickelocene half have much larger shifts than those of the cobaltocene half. MO calculations were used for further signal assignment.

Temperature-dependent proton spectra of Co′Ni″ (Fig. 4) establish the antiferromagnetic interaction between the nickelocene and the cobaltocene halves, which is discussed below. Both ^{1}H and ^{13}C NMR spectra show that after repeated recrystallization of Co′Ni″ from pentane paramagnetic and diamagnetic impurities are still present.

Cyclic voltammetry

The tetradecabimetallocenes of nickel (Ni′Ni″), cobalt ($Co'^+Co''^+$) and nickel/cobalt (Co′Ni″) underwent electron transfers (ETs) when subjected to cyclic voltammetry (CV); the results are listed in Table 1. When Ni′Ni″ was investigated in propionitrile the separation ΔE_p between the anodic and cathodic potentials (E_{pa} and E_{pc}, respectively) indicated reversible and quasi-reversible ETs. However, even at −21 °C the ETs of decomposition products complicated the analysis. Very likely, the binickelocene ions were attacked by the donor solvent, because the expected four ETs were observed only when the CV was recorded in *o*-difluorobenzene. There were also disadvantages encountered with *o*-difluorobenzene: ΔE_p values were larger, the highest oxidation was chemically not reversible, and adsorption at the electrode distorted the wave associated with the reduction of the trication. This was confirmed by changing the scan rate (v). As expected for

Table 1 Electrochemical data[a] (in mV) of the tetradecamethylbimetallocene derivatives Ni′Ni″, $Co'Co''^+$ and Co′Ni″

	$Co'Co''^+$	Co′Ni″	Ni′Ni″	Ni′Ni″[b]
$E_{1/2}(-2/-1)$	−3150			
(ΔE_p)	(170–245)			
$E_{1/2}(-1/0)$		−2040		
(ΔE_p)		(90)		
$E_{1/2}(0/1)$	−2200	−1415	−1235	−1205
(ΔE_p)	(100)	(80)	(120)	(60)
$E_{1/2}(1/2)$	−1310	−445	−685	−685
(ΔE_p)	(80)	(70)	(130)	(60)
$E_{1/2}(2/3)$		465	35[c]	15
(ΔE_p)		(170)	(210)	(80)
$E_{1/2}(3/4)$			575(E_{pa})	545
(ΔE_p)				(70)

[a] In *o*-difluorobenzene at 25 °C unless stated otherwise. Supporting electrolyte 0.1 M $[n\text{-}Bu_4N]^+[PF_6]^-$, scan rate 200 mV s^{-1}, potentials relative to $Cp_2Fe/[Cp_2Fe]^+$. [b] In propionitrile at −21 °C. [c] Disturbed by adsorption of the trication at the electrode.

adsorption[13] the peak current increased linearly with v while for the other ETs increases with $v^{1/2}$ were found.

Discussion

Rearrangement of the expected anionic nickelocene Ni′-[C_5Me_4]$^-$

As mentioned above deprotonation of Ni′-C_5Me_4H gave the anion Ni″-[C_5H_4]$^-$ instead of the expected anion Ni′-[C_5Me_4]$^-$ (Scheme 2). In order to observe the unstable primary deprotonation product Ni′-[C_5Me_4]$^-$ sodium hydride was added to Ni′-C_5Me_4H dissolved in THF-d_8 at −78 °C in an NMR tube. ^{1}H NMR spectra recorded at increasing temperatures showed that the reaction started near room temperature and that the only detectable anion was Ni″-[C_5H_4]$^-$. Reaction with n-BuLi in hexane at −78 °C was also unsuccessful while at higher temperature decomposition of Ni′-C_5Me_4H (probably analogous to that known for the parent nickelocene[14]) occurred.

In an *inter*molecular rearrangement two Ni′-[C_5Me_4]$^-$ anions would give dianion **2** and Ni′Ni″ (Scheme 1), which in turn would be transformed into two Ni″-[C_5H_4]$^-$ anions. However, pure Ni′Ni″ did not react with anions like **2** and [C_5Me_5]$^-$ so that an *intra*molecular rearrangement is more likely. A solvated intermediate [(C_5Me_5)Ni]$^+$ fragment is also conceivable. For a qualitative understanding of the rearrangement extended Hückel MO (EHMO) calculations were carried out.

Fig. 5 visualizes what happens when the [(C_5Me_5)Ni]$^+$ fragment moves (in 11 steps) across the methylated pentafulvalene dianion (**2**) following the line that connects the centers of the five-membered rings. The limiting structures are Ni′-[C_5Me_4]$^-$ and Ni″-[C_5H_4]$^-$, and midway between both structures the [(C_5Me_5)Ni]$^+$ fragment is placed above the central bond of **2**. The shift of [(C_5Me_5)Ni]$^+$ is accompanied by a change in the total energy (broken curve in Fig. 5), which is mainly determined by the singly occupied MOs 30a″ and 40a′ and by the HOMO 39a′. Lower lying MOs weakly modulate the total energy curve and are neglected in the qualitative reasoning. From Fig. 5 it follows that Ni″-[C_5H_4]$^-$ is more stable than Ni′-[C_5Me_4]$^-$ and that there is no barrier

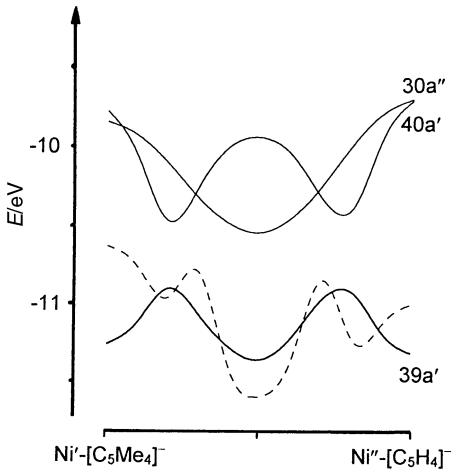

Fig. 5 Walch diagram for the shift of the [(C_5Me_5)Ni]$^+$ fragment across the tetramethylpentafulvalene dianion. Limiting structures are Ni′-[C_5Me_4]$^-$ and Ni″-[C_5H_4]$^-$. Only the most relevant MOs (see also Fig. 6) are given. The total energy is represented by a broken line.

when passing from Ni′-[C_5Me_4]$^-$ to Ni″-[C_5H_4]$^-$. The higher stability of Ni″-[C_5H_4]$^-$ is due to the methyl groups of the ligand **2**, as can be seen in the interaction diagram given in Fig. 6. Methylation pushes the orbital 18a″ of **2** to higher energy, while for the parent pentafulvalene dianion the MOs corresponding to 18a″ and 17a″ stay at lower energy. Therefore, the interaction with the 14a″ orbital of the [(C_5Me_5)Ni]$^+$ fragment stabilizes the 29a″ orbital of Ni″-[C_5H_4]$^-$ more efficiently than the 28a″ orbital of Ni′-[C_5Me_4]$^-$. Close inspection of Fig. 6 shows additional minor stabilizations (and destabilizations) of the MOs of Ni″-[C_5H_4]$^-$.

The fact that there is no energy barrier for the rearrangement Ni′-[C_5Me_4]$^-$ → Ni″-[C_5H_4]$^-$ must be ascribed to the fact that the energy changes of the HOMO 39a′ and the SOMOs 30a″ and 40a′ largely compensate each other (Fig. 5). When the nickel atom of Ni′-[C_5Me_4]$^-$ and Ni″-[C_5H_4]$^-$ is replaced with iron, the resulting anionic ferrocene Fe′-[C_5Me_4]$^-$ is again less stable than Fe″-[C_5H_4]$^-$. However, the MOs 30a″ and 40a′ are now empty, and quite expectedly,

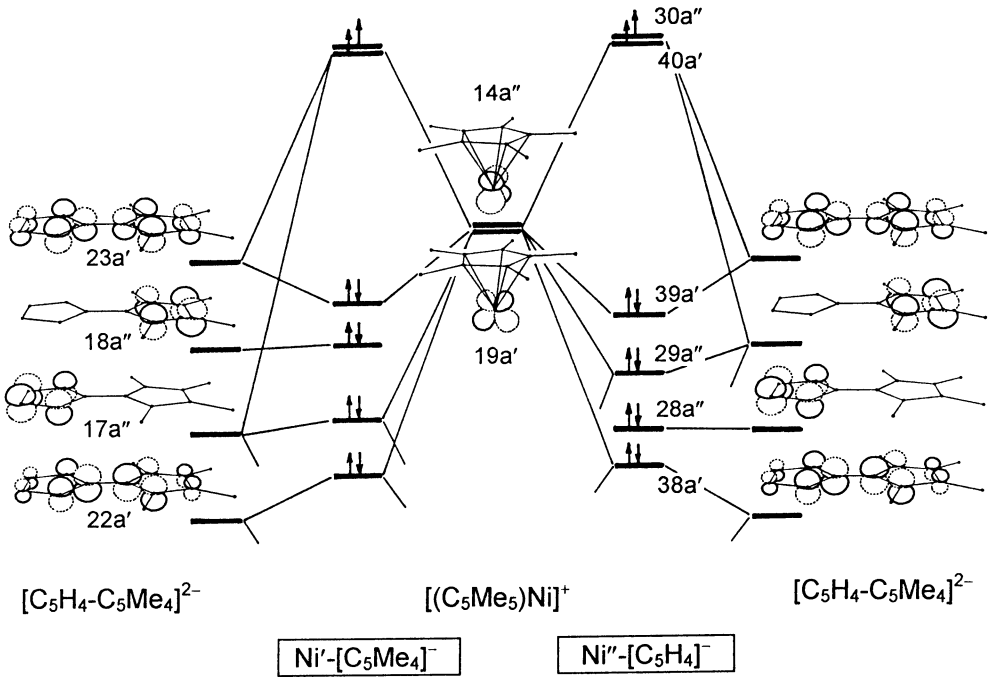

Fig. 6 MO scheme of important interactions of tetramethylpentafulvalene dianion with [(C_5Me_5)Ni]$^+$ to give the anionic nickelocenes Ni′-[C_5Me_4]$^-$ and Ni″-[C_5H_4]$^-$. The symmetry labels apply to both sides of the scheme; the electron occupation of the fragment orbitals has been omitted.

the barrier of the rearrangement Fe′-$[C_5Me_4]^-$ → Fe″-$[C_5H_4]^-$ is high. Actually, we have found that Fe′-$[C_5Me_4]^-$ is a stable species while Fe″-$[C_5H_4]^-$ could not be observed.[7b]

The reaction Ni′-$[C_5Me_4]^-$ → Ni″-$[C_5H_4]^-$ can be classified as an η^5,η^5-haptotropic rearrangement. There is a multitude of haptotropic rearrangements,[14] most of which occur on the surface of condensed π systems. The only known η^5,η^5 variant seems to have been reported for pentalenyl derivatives[15] where the metal-containing fragment moves to a new binding site at a distance of 2 Å (by choosing a detour[16]). The present study shows that the $[(C_5Me_5)Ni]^+$ fragment moves 3.9 Å, and that the narrow path of a single bond (rather than the broad avenue of a condensed π ligand) is sufficient.

Spin density distribution

The spin density ρ at a given carbon nucleus of the ligand π system of paramagnetic metallocenes is related to the corresponding squared $2p_z$ AO coefficient and to the contact shift, δ^{con}. It follows that δ^{con} is a measure of ρ. We have applied the relation previously for the determination of the spin-carrying MOs of symmetric bimetallocenes[3c,e] so that the discussion can be restricted here to a few facts. While deducing spin maps of the new compounds from NMR results, some missing signal assignments are established by comparison with EHMO calculations.

Nickelocenes Ni′-C_5Me_4H and Ni″-$[C_5H_4]$Na. Nickelocene has two unpaired electrons in a pair of degenerate orbitals. When substituted as in the case of Ni′-C_5Me_4H and Ni″-$[C_5H_4]^-$ the degeneracy is lifted, but the $S = 1$ ground state is retained. Fig. 7 displays one of the singly occupied MOs of Ni′-C_5Me_4H and Ni″-$[C_5H_4]^-$. These MOs do not only show appreciable $2p_z$ contributions—and hence spin density—at the nickelocene carbon atoms but also at some of the cyclopentadiene and cyclopentadienyl substituents. The other singly occupied MOs of Ni′-C_5Me_4H and Ni″-$[C_5H_4]^-$ (not shown) have negligibly little spin at those substituents. As for the cyclopentadiene moiety of Ni′-C_5Me_4H positive spin is only found at C_5 and C_3, and there is more spin at C_5 than at C_3 (Fig. 7). The two strongly shifted signals at high frequency were assigned accordingly. The spin in the $2p_z$ orbital of a given carbon atom is transmitted to its nearest neighbors by polarization, which implies inversion of the spin sign and hence of the NMR signal shift.[5c] Therefore, the signals of C_1 and C_4 have negative shifts. The signal shift of C_1 (−684.5 ppm) is larger than that of C_4 (−245 ppm) because there is more spin at the neighbors $C_{1'}$ and C_5 than at C_3 and C_5. Finally, the signal shift of C_2 is small (95.7 ppm), because C_2 receives negative spin from C_4 and positive spin from $C_{1'}$ and C_5 (after two polarization steps). The spin densities at C_{2-5} are also reflected in the NMR signal shifts of the nuclei of the adjacent methyl groups. On passing from C_3 and C_5 to Me_3 and Me_5 the shift signs of the carbon signals change, and the signal shift of Me_5 is larger than that of Me_3 (−204 and −119 ppm, respectively). The remaining signal, which has a quartet structure, must belong to Me_2. On further passing to the methyl protons the spin sign changes once again, while the signals of Me_5 and Me_4 are more shifted than those of Me_3 and Me_2 (see Fig. 3). The signal assignment of $H_{2'-5'}$ is not clear as now *both* SOMOs contribute to the spin distribution in such a way that the signal shifts are very similar. The assignment of the signals of Ni″-$[C_5H_4]^-$ proceeds in the same way, guided by its SOMO (Fig. 7).

The NMR signal shifts obtained from the spectra are a measure of the spin densities only after conversion to contact shifts (see Experimental), which are collected in Table 2. In summary, these data show that in the nickelocenes Ni′-C_5Me_4H and Ni″-$[C_5H_4]$Na the unpaired electrons are not restricted to the Ni′ and Ni″ moieties. Rather, there is considerable transfer to the cyclopentadiene and cyclopentadienyl substituents where characteristic spin sign patterns are produced.

Tetradecamethylbinickelocene, Ni′Ni″. The spin distribution in Ni′Ni″ corresponds to that in decamethylbinickelocene, Ni′Ni′,[3c] because, qualitatively, the same orbitals (Fig. 8) are engaged. The main difference is that MOs 43a″ and 44a″ are localized on the penta- and nonamethylated halves of Ni′Ni″, respectively, and that their energy splitting is much larger than in the case of Ni′Ni′. Both changes result from asymmetric methylation of the pentafulvalene bridge of Ni′Ni″ (see Fig. 6). These facts facilitate the signal assignment of the NMR spectra. Whatever the nucleus at positions 1–5 (and 1′–5′) of the pentafulvalene bridge, the expected signal sequence is $|1| < |3/4| < |2/5|$. The EHMO results also suggest that there is more spin at the C_5Me_5 ligand of the penta- than of the nonamethylated half of Ni′Ni″. The corresponding signals were assigned accordingly except for the five-membered ring carbon atoms whose signals are not resolved. The interactions within Ni′Ni″ are discussed below.

Tetradecamethylbicobaltocenium cation, Co′Co″$^+$. This compound has only one unpaired electron, and is hence particularly well suited for checking the qualitative MO approach to the correlation between NMR results and spin distribution. The shapes of the important MOs of Co′Co″$^+$ are the same as those of Ni′Ni″ (Fig. 8). The lowest-energy MO, 58a′, is singly occupied, and the signal sequence of all nuclei of the pentafulvalene bridge is expected to be $|1| < |3/4| < |2/5|$ and

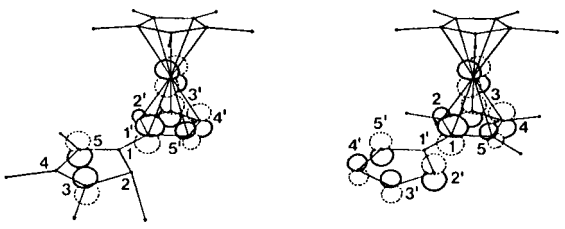

Fig. 7 Selected singly occupied MOs of Ni′-C_5Me_4H (left) and Ni″-$[C_5H_4]^-$ (right) reflecting the NMR signal patterns (see text). For clarity no protons and only relevant AO contributions (Ni, C_{1-5}, $C_{1'-5'}$) are shown.

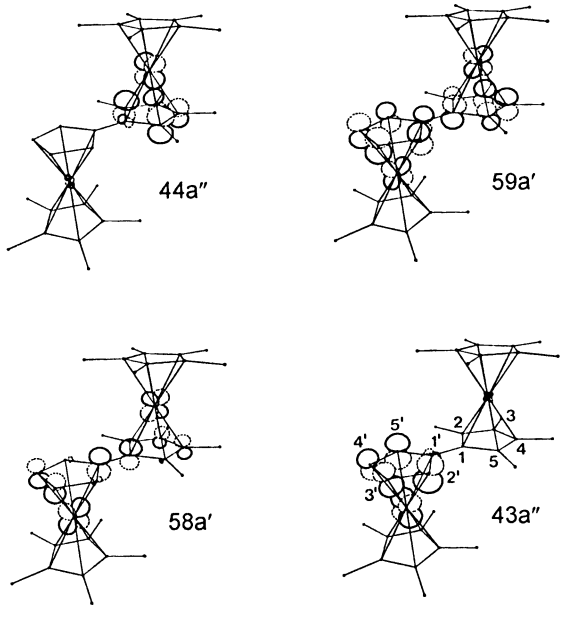

Fig. 8 MOs of Ni′Ni″ important for spin distribution. For clarity no protons and only relevant AO contributions (Ni, C_{1-5}, $C_{1'-5'}$) are shown.

Table 2 ^{1}H and ^{13}C contact shifts of the nickelocene derivatives Ni′-C_5Me_4H and Ni″-[C_5H_4]Na and the tetradecamethylbimetallocene derivatives Ni′Ni″, [Co′Co″$^+$][PF_6]$^-$ and Co′Ni″

Nucleus and position	Ni′-C_5Me_4H	Ni″-[C_5H_4]Na	Ni′Ni″	[Co′Co″$^+$][PF_6]$^-$	Co′Ni″
^{1}H NMR					
T/K	298	298	300	310.7	310.7
C_5Me_5 (nona[a])		228	103.30	7.0	178.1
C_5Me_5 (penta[b])	248		108.0	25.3	11.7
$H_{2'/5'}$	210, 213[c]	−26.6	−109.2	13.9	−17.9
$H_{3'/4'}$	213, 216[c]	−8.8	−82.7	−12.9	−51.4
$Me_{2/5}$	−2.7, 115.1	263[d]	118.0	−1.2	139.2
$Me_{3/4}$	75.3, −25.0	252[d]	88.3	−10.2	170.3
H_2	24.5				
^{13}C NMR					
T/K	298	298	369.3	332	332
C_5Me_5 (nona[a])[e]	670	80	1048		
C_5Me_5 (penta[b])	[e]		669	304	207
C_5Me_5 (nona[a])		−624	−260	−28.2	−416
C_5Me_5 (penta[b])	−749		−301	−96.8	−56.7
$C_{1'}$	[e]	−697	304[f]	304	−607
$C_{2'/5'}$	[e]	400	842	−77.2	787.9
$C_{3'/4'}$	[e]	18.1	592[g]	235	579
C_1	−976	[e]	272[f]	117	1164
$C_{2/5}$	52.2, 811	[e]	836	−98.0	943
$C_{3/4}$	394, −465	[e]	467[g]	37.4	940
$Me_{2/5}$	40.1, −263	−675[d]	−289	126.7	−392
$Me_{3/4}$	−159, 251	−661[d]	−245	8.6	−538

[a] Nonamethylmetallocenyl. [b] Pentamethylmetallocenyl. [c] Two coinciding signals, assignment of $H_{2'-5'}$ unclear. [d] Interchange of $Me_{2/5}$ and $Me_{3/4}$ not excluded. [e] Signal-to-noise too low. [f] Interchange of $C_{1'}$ and C_1 not excluded. [g] Interchange of $C_{3'/4'}$ and $C_{3/4}$ not excluded.

$|1'| < |3'/4'| < |2'/5'|$. These patterns were established by the ^{13}C NMR spectrum (Fig. 2), and the ^{1}H NMR signals were assigned accordingly.

Because the EHMO energies are not very reliable, the thermal accessibility of the LUMO of Co′Co″$^+$ (MO 43a″ in Fig. 8) was investigated experimentally. Population of MO 43a″ would imply that the reduced paramagnetic contact shifts $\vartheta_{298} = \delta^{con}\ T/T_s$ (T and T_s are the measuring and standard temperatures, respectively; here $T_s = 298$ K) are no longer constant with T, because the spin density at $C_{1'}$ and $C_{3'/4'}$ increases while it decreases at $C_{2'/5'}$. For Co′Co″$^+$ one would expect that the magnitude of $\vartheta_{298}(^1H_{3'/4'})$ increases and that of $\vartheta_{298}(^1H_{2'/5'})$ decreases while all other ϑ_{298} values remain nearly constant. Although these trends are observed experimentally (Fig. 9), they are weak and within the error limits that are introduced by the calculated dipolar signal shifts (see Experimental). We conclude that the population of MO 43a″ is marginal (>0.1 eV above the HOMO) and that it would hardly influence the evaluation of the magnetic exchange described below for Ni′Ni″ and Co′Ni″, which have similar MO splittings.

The cation Co′Co″$^+$ resembles the anionic nickelocene Ni″-[C_5H_4]$^-$ in that much spin is transferred from a paramagnetic metallocene to an adjacent cyclopentadienyl moiety, which has no proper spin source. This is reflected in large contact shifts for $C_{1'-5'}$ of both compounds (Table 2). However, different MOs are responsible for the spin distribution (see right hand side of Fig. 7 and MO 58a′ in Fig. 8) so that the signal shift patterns are also different. In addition, contact shifts were found for the ^{1}H and ^{13}C NMR signals of C_5Me_5 of the nonamethylated cobaltocenium half of Co′Co″$^+$. This means that the unpaired electron is delocalized across the 18-electron cobalt center to the remote C_5Me_5 ligand.

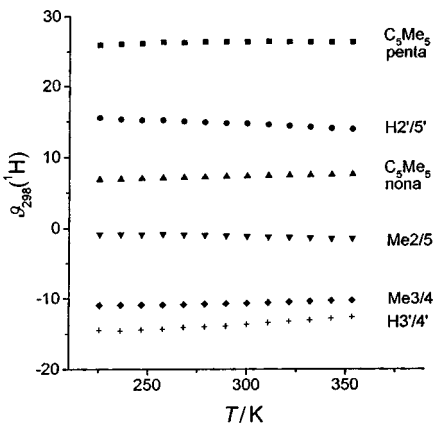

Fig. 9 Temperature dependence of the reduced ^{1}H NMR signal shifts of [Co′Co″$^+$][PF_6]$^-$.

Cobalt/nickel tetradecamethylbimetallocene, Co′Ni″. There are two approaches to the understanding of Co′Ni″. (i) MO 58a′ in Fig. 8 might be doubly occupied, and one unpaired electron in MO 43a″ would be responsible for the spin distribution. (ii) The spin distribution is the sum of that produced by the cobaltocene and nickelocene halves. The first approach would imply that there is no spin at the nickelocene ligands, because the SOMO, 43a″, is localized on the cobaltocene half. This is excluded by the NMR spectra, which show strongly shifted signals for both the cobaltocene and nickelocene halves (Fig. 4 and SI 4). Instead, the second approach is supported by the NMR data given in Table 2: when the contact shifts of Ni″-[C_5H_4]$^-$ and Co′Co″$^+$ are added, the spin pattern and the relative amount of the spin at most nuclei of Co′Ni″ is reproduced. Of course, there is no quantitative agreement as Ni″-[C_5H_4]$^-$ and Co′Co″$^+$ are not perfect models for the two halves of Co′Ni″ and as an antiferromagnetic interaction occurs.

Magnetic interaction

It has been shown previously that the magnetic interaction constant J of Ni′Ni′ can be determined by fitting the temperature-dependent NMR signal shifts.[3c] The general fitting function adapted[17] to our problems is

$$\vartheta_{298} = \sum_j \frac{\vartheta_{\infty j}}{S_j(S_j+1)} \frac{\sum_j c_{ij} S_i'(S_i'+1)(2S_i'+1)\exp(E_i/kT)}{\sum_i (2S_i'+1)\exp(E_i/kT)} \quad (1)$$

where j runs over the engaged paramagnetic moieties with spin S_j, and i runs over the energy levels $E_i = J/2[S'_i(S'_i+1) - \sum_j S_j(S_j+1)]$ (with spin S'_i) obtained in the Dirac–Heisenberg–Van Vleck model. The reduced contact shift, ϑ_{298}, mentioned above adopts a limiting value, ϑ_∞, at infinite temperature, c_{ij} are tabulated[17] coefficients, k is the Boltzmann constant, and T is the absolute temperature. ϑ_∞ is an instructive parameter, because it is the reduced shift that would be obtained if the molecule had magnetically independent moieties, that is the shifts that are known from similar mononuclear compounds. For the bimetallocenes Ni′Ni″ and Co′Ni″, eqn. (1) yields two terms. In the case of Ni′Ni″ the two exponential terms are identical so that sums of the limiting signal shift contributions of a given nickelocene and its adjacent nickelocene result, and eqn. (1) becomes

$$\vartheta_{298} = \frac{3}{2}(\vartheta_{\infty,\,\mathrm{Ni}'} + \vartheta_{\infty,\,\mathrm{Ni}''})\,\frac{\exp(J/kT) + 5\exp(3J/kT)}{1 + 3\exp(J/kT) + 5\exp(3J/kT)} \qquad (2)$$

while for Co′Ni″ eqn. (1) takes the form

$$\vartheta_{298} = \frac{1}{2}\vartheta_{\infty,\,\mathrm{Ni}''}\,\frac{5\exp(3J/2kT) - 1/2}{2 + 4\exp(3J/2kT)} + \frac{3}{4}\vartheta_{\infty,\,\mathrm{Co}'}\,\frac{5\exp(3J/2kT) + 1}{1 + 2\exp(3J/2kT)} \qquad (3)$$

When paramagnetic compounds follow the Curie law, ϑ_{298} is constant with T. The reduced proton NMR signal shifts of the bimetallocenes deviate from this behavior as shown in Fig. 10. Fitting of the experimental data to eqn. (2) and (3) gave the curves in Fig. 10 and the parameters listed in Table 3. The J values vary somewhat depending on the ^{1}H NMR signal used. In the case of Ni′Ni″ the mean value $J = -195$ cm^{-1} indicates that the antiferromagnetic interaction is more efficient than in Ni′Ni′ ($J = -180$ cm^{-1}[3c]) while the limiting signal shifts ϑ_∞ are in ranges expected for simple nickelocenes [*e.g.*, $\vartheta_{298}(^1\mathrm{H}) = -257$ and 240 for Cp_2Ni and $(C_5Me_5)_2Ni$, respectively].

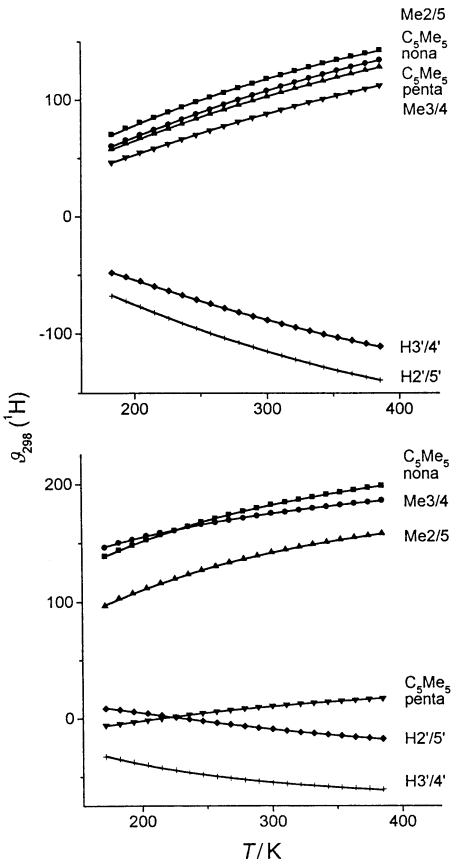

Fig. 10 Temperature dependence of the reduced ^{1}H NMR signal shifts of Ni′Ni″ (top) and Co′Ni″ (bottom). Curves through the experimental points were obtained by fitting the data to eqn. (2) and (3), respectively.

Table 3 Magnetic exchange parameters (J) and limiting signal shifts (ϑ_∞) of Ni′Ni″ and Co′Ni″ obtained by fitting temperature-dependent ^{1}H NMR data

Signal used for fit	J/cm^{-1}	$\vartheta_\infty(^1\mathrm{H})^a$/ppm
Ni′Ni″		
$Me_{2/5}$	−170	
C_5Me_5 (nona)	−196	258
C_5Me_5 (penta)	−196	246
$Me_{3/4}$	−223	240
$H_{3'/4'}$	−209	−225
$H_{2'/5'}$	−173	−246
Co′Ni″		
C_5Me_5 (nona)	−174	188
$Me_{3/4}$	−178	65
$Me_{2/5}$	−169	240
C_5Me_5 (penta)	−207	126
$H_{2'/5'}$	−243	−141
$H_{3'/4'}$	−103	−220

[a] Sum of the limiting shifts of both metallocenes.

The fit of the ^{1}H NMR data of Co′Ni″ was less good as can be seen from the larger scatter of the J values. The scatter is most obvious for the J values derived from the signals of C_5Me_5 penta, $H_{2'/5'}$ and $H_{3'/4'}$. A better fit was obtained when it was restricted to the data of C_5Me_5 (nona), $Me_{3/4}$ and $Me_{2/5}$. The mean J value was then $J = -174$ cm^{-1}, which is, nevertheless, close to that obtained from the fit of all proton data ($J = -179$ cm^{-1}). The ϑ_∞ values of C_5Me_5 (nona) and $Me_{2/5}$ are not far from the sum of the nickelocene and cobaltocene contributions taken from Ni″[C_5H_4]Na and [Co′Co″$^+$][PF_6]$^-$, respectively (Table 2). We have also explored the inclusion of dipolar shifts in the fitting model. However, this contribution is negligibly small, because we are dealing with protons that are rather distant from the spin center. The same applies when nickelocene fragments are engaged, even though zero field splitting and an additional temperature dependence come into play. We have no explanation for the special behavior of the curve of $Me_{3/4}$ in Fig. 10, which is obviously associated with the low value of $\vartheta_\infty(Me_{3/4})$ in Table 3.

Redox behavior

The redox potentials of the new asymmetric bimetallocenes Ni′Ni″, Co′Co″ (investigated as [Co′Co″$^+$][PF_6]$^-$), and Co′Ni″ have characteristic features that become obvious, when they are compared with those of (C_5Me_5)CoCp (Co′), (C_5Me_5)NiCp (Ni′), Co′Co′ and Ni′Ni′ reported previously.[3e] An overview is given in Fig. 11, where the discussion starts with Co′ and Ni′. Formal coupling of these metallocenes gives the bimetallocenes Co′Co′ and Ni′Ni′, respectively, and this in turn leads to a potential splitting. The potential of the ET of Co′Co′/Co′Co′$^+$ is lowered relative to that of Co′/Co′$^+$ owing to charge delocalization in Co′Co′$^+$ while the potential of the ET of Co′Co′$^+$/Co′$^+$Co′$^+$ is higher owing to the repulsion of two charges in Co′$^+$Co′$^+$. The same is true for the reduction of Co′Co′ and the stepwise oxidation of Ni′Ni′, although the potentials are modulated somewhat, because the electrons are added to and removed from different orbitals.

Next we pass from M′M′ to M′M″. This is accompanied by a lowering of the potentials of the ETs of Co′Co″/Co′Co″$^+$ and of Ni′Ni″/Ni′Ni″$^+$. For the nickel compounds the potential shift is 210 mV, which would be expected from the elec-

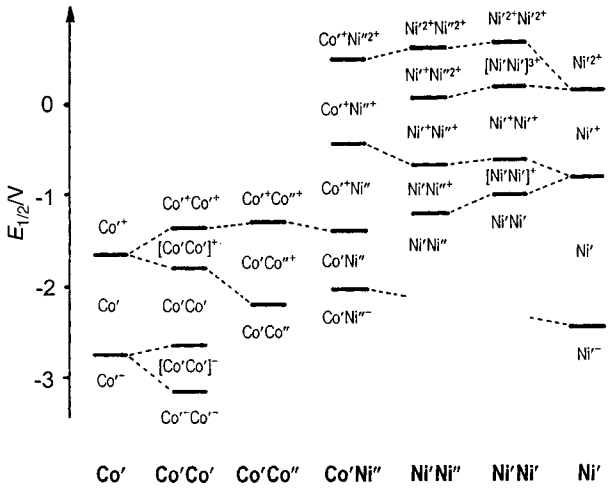

Fig. 11 Comparison of the redox potentials of the asymmetric bimetallocenes Co′Co″, Co′Ni″ and Ni′Ni″ with those of the symmetric bimetallocenenes Co′Co′ and Ni′Ni′ and with the pentamethylmetallocenes Co′ and Ni′. The species existing between the potentials are indicated.

tron releasing power of four additional methyl groups[18] in Ni′Ni″ as compared to Ni′Ni′. Actually, this result must be regarded as accidental, because charge localization in Ni′Ni″$^{+}$ should increase the potential as compared to the delocalized Ni′Ni′$^{+}$, while different solvation might lower the potential. It is, therefore, no surprise that for the corresponding cobalt species the potential shift is different (400 mV). On the other hand, in the bimetallocene series there is little change in the ET potentials that lead to symmetrically charged species of the type M′$^{+}$M″$^{+}$ and M′$^{2+}$M″$^{2+}$. We conclude that these potentials are mainly determined by the interaction of equal charges on adjacent metallocenes, which should be fairly constant.

All redox potentials found for Co′Ni″ must be assigned to localized ETs. Thus, the ETs at 465, −445 and −1415 mV belong to the oxidations of the fragments Ni″, Ni″$^{+}$ and Co′, respectively, while the ET at −2040 mV belongs to the reduction of the Ni″ fragment. The ETs are related to those of the other cobaltocene and nickelocene derivatives included in Fig. 11 as indicated by broken lines.

Conclusions

A broadly applicable strategy of lowering the symmetry of bimetallocenes consists of methylating one half of the bridging pentafulvalene ligand. When bimetallocenes are asymmetric and when they contain charges and/or unpaired electrons both can be localized on one of the two metals. For instance, in the tetradecamethylbicobaltocenium monocation, Co′Co″$^{+}$, the positive charge is localized on the cobalt atom of the nonamethylated half (Co″), while the unpaired electron is localized on the cobalt atom of the pentamethylated half (Co′). Another interesting aspect of symmetry lowering is that mixed-metal bimetallocenes are accessible. An example is Co′Ni″ where one and two spins are localized largely on the cobalt and nickel atoms, respectively.

The method of choice to prove this is NMR spectroscopy. It also shows that the unpaired electrons are partly delocalized up to the most distant ^{1}H and ^{13}C nuclei of seemingly diamagnetic fragments of a bimetallocene. MO calculations are helpful for analyzing details of the spin distribution in all paramagnetic molecules of this work. A consequence of spin delocalization is magnetic interaction between two paramagnetic halves of bimetallocenes. Temperature-dependent NMR studies can be used to quantitatively determine antiferromagnetic coupling, which increases when the bridging pentafulvalene ligand is methylated. There are also interactions between the charges of oxidized bimetallocenes, which follows from the splitting of redox potentials seen in the cyclic voltammograms.

An unusual rearrangement has been discovered with a nickelocene that is linked to a cyclopentadienyl anion: the $(C_5Me_5)Ni^{+}$ fragment undergoes a haptotropic shift from the non-methylated to the tetramethylated half of pentafulvalene dianion. MO calculations show that this is due to two electrons in two quasi-degenerate antibonding orbitals.

Experimental

Methods and materials

All preparative work and characterization of the new compounds were carried out under oxygen- and moisture-free dinitrogen by using dry solvents and standard Schlenk equipment. For adding and decanting solvents as well as for filtration the canula technique was employed. UV/vis spectra were recorded on a Perkin-Elmer Lambda 2 spectrometer. Mass spectra were obtained from a Finnigan MAT 90 apparatus working in the electron impact mode at 70 eV. For cyclic voltammetry measurements an EG&G Princeton Applied Research 173/276 potentiostat was used. Home-made cells were equipped with a small column for final drying of the solvent over activated Al_2O_3, with platinum wire working and counter electrodes, and with an Ag/AgCl reference electrode. $[n\text{-}Bu_4N]^{+}[PF_6]^{-}$ (0.1 molar in propionitrile) served as supporting electrolyte. The potentials were referenced relative to that of internal $[Cp_2Co]^{+}[PF_6]^{-}$ and calculated relative to the couple $[Cp_2Fe]^{0/+1}$.

NMR spectra were recorded on a Bruker MSL 300 spectrometer (^{1}H 300.13, ^{13}C 75.47 MHz) by using tubes equipped with ground glass fittings and stoppers. For ^{13}C NMR spectra solenoid coils and specially designed tubes described previously were used.[19] The sample temperature was determined by calibration with ethylene glycol; all diamagnetic samples were measured at 305 K. Experimental shifts of paramagnetic compounds at the measuring temperature T (δ_T^{exp}) were determined relative to solvent signals and calculated relative to TMS by using tabulated data.[20] The multiplicity given with ^{13}C NMR signals refers to $^{1}J_{C,H}$ couplings unless stated otherwise. The δ_T^{exp} values were converted to paramagnetic shifts, δ_T^{para}, by subtracting the corresponding signal shift of analogous ferrocenes[7b] and of $[Co'^{+}Co''^{+}][PF_6]^{-}{}_2$. Contact shifts, δ_T^{con}, were obtained after subtracting the dipolar signal shifts, δ_T^{dip}, from δ_T^{para}. The δ_T^{dip} values were calculated previously for the Co′ and Ni′ halves of bimetallocenes.[3e] The same values were obtained for the Ni″ moiety within the error limits. Magnetic interaction was taken into account by considering that it acts on δ_T^{dip} through the term $S(S+1)$ and that the proportionality $\vartheta_T \propto S(S+1)$ holds.[21] For Ni′Ni″ it was calculated from eqn. (2) and $J = -195$ cm^{-1} that ϑ_{300} is smaller than ϑ_∞ by a factor of 0.41. Therefore, δ_{300}^{dip} was reduced by the same factor. In the case of Co′Ni″ eqn. (3) and $J = -174$ cm^{-1} yielded factors of 0.78 and 0.31 by which the δ_{311}^{dip} values of the Co′ and Ni″ moieties, respectively, were reduced.

For the MO calculations the program CACAO, version 4.0[22] was utilized. Mean atomic distances were taken from representative crystal structures,[23] and idealized angles were used.

The following reagents and starting compounds were prepared as described previously: 1,2,3,4-tetramethylpentafulvalene-1,5-diyldilithium,[7a] (**2**Li$_2$), 4,8-dihydro-1,2,3,4-tetramethylpentafulvalenene-8-yllithium,[7b] (**3**Li), (C_5Me_5)Ni(acac)[8] and (C_5Me_5)Co(acac).[8] Elemental analyses were carried out by the Microanalytical Laboratory of the authors' institution.

Syntheses

Pentamethyl-1′-(nonamethylnickelocen-1-yl)nickelocene (Ni′Ni″). A 1.30 g amount of the dilithium salt of **2** (6.56 mmol) was added to a stirred solution of (C_5Me_5)Ni(acac) (2.80 g, 9.55 mmol) in 200 mL of THF that had been cooled to −78 °C. The initially dark red solution was stirred for 18 h while being allowed to warm to room temperature. The resulting dark violet mixture was evaporated to dryness and the remaining solid was extracted with 100 mL of pentane by using a Soxhlet apparatus. Removal of pentane gave 2.33 g of Ni′Ni″ as a shiny black powder (yield 86% based on **2**). A repeatedly recrystallized (pentane) sample was used for elemental analysis. MS: *m/z* (%, [ion]) 571 (100, $[M]^+$), 435 (26, $[M-(C_5Me_5)]^+$), 379 (19, $[M-(C_5Me_5)Ni]^+$), 286 (100, $[M]^{2+}$), 193 (13, $[(C_5Me_5)Ni]^+$). Anal. found: C, 71.98; H, 8.18; Ni, 18.77; calc. for $C_{34}H_{46}Ni_2$: C, 71.38; H, 8.10; Ni, 20.52%. ^{1}H NMR (toluene-d_8, 300.0 K): δ^{exp}/W in Hz 119.0/360 (6H, $Me_{2/5}$), 108.6/320 (15H, C_5Me_5, nonamethylnickelocenyl), 103.8/320 (15H, C_5Me_5, pentamethylnickelocenyl), 89.0/220 (6H, $Me_{3/4}$), −84.1/370 (2H, $H_{3'/4'}$), −110.1/470 (2H, $H_{2'/5'}$). ^{13}C NMR (toluene-d_8, 369.3 K): δ^{exp}/W in Hz 897/6500 ($C_{2/5}$ and $C_{2'/5'}$), 732/3500 (2 × C_5Me_5), 647/2000 and 530/1700 ($C_{3/4}$ and $C_{3'/4'}$), 379/1800 and 343/1600 (C_1 and $C_{1'}$), −237/400 ($Me_{3/4}$), −253/370 (C_5Me_5), −278/480 ($Me_{2/5}$), −292/420 (C_5Me_5).

Pentamethylcyclopentadienyl(2′,3′,4′,5′-η⁴-2,3,4,5-tetramethylpentafulvalene)cobalt (Co′-C_5Me_4). (C_5Me_5)Co(acac) (1.96 g, 6.68 mmol) was reacted with **2** (0.69 g, 3.48 mmol) as described in the previous section. In the course of 12 h the color of the reaction mixture changed from brown to violet and eventually to dark blue. Removal of THF *in vacuo*, extraction of the solid with 100 mL of hexane and removal of the solvent gave 0.61 g of Co′C_5Me_4 as a blue–black powder (yield 46% based on **2**). MS: *m/z* (%, [ion]) 378 (100, $[M]^+$), 363 (95, $[M-Me]^+$), 347 (17, $[M-2Me]^+$), 189 (18, $[M]^{2+}$). ^{1}H NMR (C_6D_6): δ 1.33 (s, 15H, C_5Me_5), 2.31 and 2.44 (both s, 6H, $Me_{2/5}$ and $Me_{3/4}$), 4.20 and 4.52 (both AA′BB′, $^3J_{H,H} + {}^4J_{H,H} = 4.2$ Hz, 2H, $H_{2'/5'}$ and $H_{3'/4'}$). ^{13}C NMR (C_6D_6): δ 9.2 (q, C_5Me_5), 12.5 and 16.0 (both q, $Me_{2/5}$ and $Me_{3/4}$), 68.0 and 78.9 (both d, $C_{2'/5'}$ and $C_{3'/4'}$), 119.9 (s, $C_{2/5}$ or $C_{3/4}$), 120.5 (s, $C_{1'}$), signals of $C_{3/4}$ (or $C_{2/5}$) and C_1 not detected.

Pentamethyl-1′-(nonamethylcobaltocenium-1-yl)cobaltocenium bis(hexafluorophosphate) ([Co′⁺Co″⁺][PF_6]⁻₂). To a stirred solution of **2** (0.42 g, 2.1 mmol) in 150 mL of THF was added at room temperature 1.17 g (4.0 mmol) of solid (C_5Me_5)Co(acac) to give a dark brown mixture. Subsequently, solid $AgNO_3$ (4.99 g, 29.4 mmol) was added and the mixture was stirred for 12 h. The solvent was removed from the resulting orange–brown solution and the black precipitate (Ag), 200 mL of water was added and silver was filtered off from the brown solution. Addition of NH_4PF_6 (3.93 g, 24.1 mmol) gave a cloudy dark yellow precipitate and a light green solution. The solid was separated by filtration, washed with 50 mL of water, dried *in vacuo* and extracted with acetonitrile. The solvent was removed and the solid recrystallized from acetone to give 1.61 g of $[Co'^+Co''^+][PF_6]_2^-$ as yellow powder that contained two molecules of acetone per formula unit (yield 89% based on **2**). Anal. found: C, 48.95; H, 6.06; calc. for $C_{40}H_{58}Co_2F_{12}O_2P_2$: C, 49.10; H, 5.79%. ^{1}H NMR (CD_3CN): δ 1.50 (s, 15H, C_5Me_5, nonamethylcobaltocenylium), 1.81 (s, 15H, C_5Me_5, pentamethylcobaltocenylium), 1.85 and 2.01 (both s, 6H, $Me_{2/5}$ and $Me_{3/4}$), 5.44 and 5.65 (both AA′BB′, $^3J_{H,H} + {}^4J_{H,H} = 4.4$ Hz, 2H, $H_{3'/4'}$ and $H_{2'/5'}$, respectively). ^{13}C NMR (acetone-d_6): δ 8.4 (q, $^1J_{C,H} = 128$ Hz, C_5Me_5, nonamethylcobaltocenylium), 8.8 (q, $^1J_{C,H} = 130$ Hz, $Me_{2/5}$ or $Me_{3/4}$), 10.3 (q, $^1J_{C,H} = 128$ Hz, C_5Me_5, pentamethylcobaltocenylium), 12.3 (q, $^1J_{C,H} = 128$ Hz, $Me_{3/4}$ or $Me_{2/5}$), 84.8 (d, ψq, $^1J_{C,H} = 182$ Hz, $^{2,3}J_{C,H} = 6.2$ Hz, $C_{3'/4'}$), 89.8 (d, ψq, $^1J_{C,H} = 185$ Hz, $^{2,3}J_{C,H} = 6.2$ Hz, $C_{2'/5'}$), 86.3 (s, C1), 94.9 ($C_{2/5}$ or $C_{3/4}$), 95.3 (s, $C_{1'}$), 97.2 (s, C_5Me_5, nonamethylcobaltocenylium), 99.6 (s, C_5Me_5, pentamethylcobaltocenylium), 100.1 (s, $C_{3/4}$ or $C_{2/5}$).

Pentamethyl-1′-(nonamethylcobaltocenium-1-yl)cobaltocene hexafluorophosphate ([Co′Co″⁺][PF_6]⁻). A dark brown mixture obtained as described in the previous section from (C_5Me_5)Co(acac) (0.42 g, 2.1 mmol) and **2** (1.17 g 4.0 mmol) in 150 mL of THF was treated with 0.27 g (0.82 mmol) of $[Cp_2Fe]^+[PF_6]^-$. After stirring for 12 h the solvent was removed under reduced pressure and the solid was extracted with 200 mL of hexane. The resulting dark solid was separated from the black–brown solution by filtration, washed with hexane and poured into 100 mL of acetonitrile under stirring. A white solid settled from the green solution when the stirrer was switched off. When the solution was decanted and evaporated to dryness 0.44 g of $[Co'Co''^+][PF_6]^-$ was obtained as a dark green powder (yield 74% based on $[Cp_2Fe]^+[PF_6]^-$). MS: *m/z* (%, [ion]) 378 (2, $[M]^+$), 186 (100, $[LH_2]^+$), 171 (57, $[L-Me]^+$), 156 (35, $[L-2Me]^+$), 136 (48, $[C_5Me_5]^+$), 121 (80, $[C_5HMe_4]^+$), 105 (37, $[C_8H_9]^+$); L = tetramethylfulvalenediyl. Anal. found: C, 57.06; H, 6.58; calc. for $C_{34}H_{46}Co_2F_6P$: C, 56.91; H, 6.46%. ^{1}H NMR (CD_3CN, 310.7 K): δ^{exp}/W in Hz 25.4/180 (15H, C_5Me_5, pentamethylcobaltocenyl), 15.4/150 (2H, $H_{2'/5'}$), 8.4/35 (15H, C_5Me_5, nonamethylcobaltocenylium), 1.0/30 (6H, $Me_{2/5}$), −7.9/40 (6H, $Me_{3/4}$), −10.7/185 (2H, $H_{3'/4'}$). ^{13}C NMR (CD_3CN, 342.6 K): δ^{exp}/W in Hz 340/2200 (C_5Me_5, pentamethylcobaltocenyl and $C_{1'}$), 270/600 ($C_{3'/4'}$), 190/190 (C_1), 169/300 (C_5Me_5, nonamethylcobaltocenylium), 131.1/140 ($C_{2/5}$), 124.3/130 ($Me_{3/4}$), 18.3 (q, $^1J_{C,H} = 125 \pm 14$ Hz, $Me_{2/5}$), 9.5 (d, $^1J_{C,H} = 97 \pm 14$ Hz, $C_{2'/5'}$), −12.1 (sh, $C_{3'/4'}$), −16.9 (q, $^1J_{C,H} = 125 \pm 14$ Hz, C_5Me_5, nonamethylcobaltocenylium), −77.2/450 (C_5Me_5, pentamethylcobaltocenyl).

Pentamethyl-1′-(2,3,4,5-tetramethylcyclopenta-1,3-dien-1-yl)-nickelocene (Ni′-C_5Me_4H). A dark red solution of (C_5Me_5)Ni(acac) (2.45 g, 8.4 mmol) in 200 mL of THF was cooled to −78 °C, and 1.71 g (8.9 mmol) of **3**Li was added. When the mixture was stirred for 12 h and allowed to reach room temperature the color changed to green. The solvent was removed and the solid extracted in a Soxhlet apparatus with 100 mL of pentane. Removal of pentane gave 2.91 g of Ni′-C_5Me_4H as a dark green powder [yield 92% based on (C_5Me_5)Ni(acac)]. ^{1}H NMR (C_6D_6, 298 K): δ^{exp}/W in Hz 246.3/600 (15H, C_5Me_5), 117.0/130 (3H, Me_5), 77.2/70 (3H, Me_3), 28.2/60 (1H, H_2), −0.5/50 (3H, Me_2), −23.1/30 (3H, Me_4), −201/800, −205/1300 and −207/800 (1H, 2H, 1H, $H_{2'5'}$). ^{13}C NMR (toluene-d_8, 363.4 K): δ^{exp}/W in Hz 800/2400 (C_5), 458/1100 (C_3), 217.0/750 (Me_4), 95.7 (d, C_2), 50.9 (q, Me_2), −119 (q, Me_3), −204.2/660 (Me_5), −246/950 (C_4), −610/1000 (C_5Me_5); for signals of C_5Me_5 and $C_{1'-5'}$ see text.

Pentamethyl-1′-(2,3,4,5-tetramethylcyclopenta-1,3-dien-1-yl)-nickelocen-5-yl sodium (Ni″-[C_5H_4]Na). To a green solution of Ni′-C_5Me_4H (1.65 g, 4.35 mmol) in 200 mL of THF was added 0.25 g (10.4 mmol) of NaH. After stirring for 12 h at ambient temperature a brown–green mixture was obtained. Excess NaH was filtered off, THF was removed *in vacuo* and the remainder was washed with 50 mL portions of hexane until the solvent was colorless. Drying of the solid *in vacuo* gave 1.4 g of Ni″-[C_5H_4]Na as a brown–green powder. The calculated yield is 84% based on Ni′-C_5Me_4H; owing to an impurity detected by ^{13}C NMR spectroscopy it is actually somewhat lower. ^{1}H NMR (DMSO-d_6, 298 K): δ^{exp}/W in Hz 261/1050 and 250/950 (both 6H, $Me_{2/5}$ and $Me_{3/4}$), 226/850 (15H, C_5Me_5), −5.6/40 (2H, $H_{3'/4'}$), −23.0/180 (2H, $H_{2'/5'}$).

^{13}C NMR (THF, 298 K): δ^{exp}/W in Hz 465/800 ($C_{2'/5'}$), 86.5 (d, $^{1}J_{C,H} = 140 \pm 14$ Hz, $C_{3'/4'}$), −590/800 ($C_{1'}$), −621/1000 (C_5Me_5), −656/1100 and −667/1200 ($Me_{2/5}$ and $Me_{3/4}$); for signals of C_5Me_5 and C_{1-5} see text.

Pentamethyl-1′-(nonamethylnickelocen-1-yl)cobaltocene (Co′Ni″). To a stirred solution of Ni″-[C_5H_4]Na (1.0 g, 2.49 mmol) in 200 mL of THF was added at room temperature 0.67 g (2.28 mmol) of (C_5Me_5)Co(acac). The onset of the reaction was indicated by a color change from brown–green to brown. After stirring overnight the solvent was stripped and the dark solid extracted with 200 mL of hexane. Reducing the volume of the dark green solution to 50 mL and cooling to −78 °C gave a precipitate, which after filtering and drying *in vacuo* gave 0.2 g of Co′Ni″ as a black–green powder [yield 15% based on (C_5Me_5)Co(acac)]. NMR spectroscopy disclosed signals of diamagnetic impurities so that the actual yield was somewhat lower. MS: *m/z* (%, [ion]) 572 (2, $[M]^+$), 435 (2, $[M - (C_5Me_5)]^+$), 377 (9, $[M - (C_5Me_5)Co]^+$), 192 (34, $[(C_5Me_5)Ni]^+$), 135 (100, $[C_5Me_5]^+$), 119 (92, $[C_9H_{11}]^+$), 105 (45, $[C_8H_9]^+$). ^{1}H NMR (toluene-d_8, 310.7 K): δ^{exp}/W in Hz 178.6/390 [15H, (C_5Me_5)Ni], 171.0/400 (6H, $Me_{3/4}$), 140.1/260 (6H, $Me_{2/5}$), 12.8/30 [15H, (C_5Me_5)Co], −6.0/60 (2H, $H_{2'/5'}$), −50.1/110 (2H, $H_{3'/4'}$). ^{13}C NMR (THF, 332.0 K): δ^{exp}/W in Hz 1243/2000 (C_1), 1113/3500 [(C_5Me_5)Ni], 1006/6500 ($C_{2/5}$ and $C_{3/4}$), 641/1700 ($C_{3'/4'}$), 277/1600 [(C_5Me_5)Co], 148/1800 ($C_{2'/5'}$), −49.5/400 [(C_5Me_5)Co], −381.0/370 ($Me_{2/5}$), −428.9/480 [(C_5Me_5)Ni], −529.7/420 ($Me_{3/4}$), −547.8/420 ($C_{1'}$).

Acknowledgement

This work has been supported by the Deutsche Forschungsgemeinschaft and the Fonds der Chemischen Industrie.

References

1 (*a*) O. Kahn, *Acc. Chem. Res.*, 2000, **33**, 647; (*b*) J. S Miller, *Inorg. Chem.*, 2000, **39**, 4392; (*c*) M. Verdaguer, A. Bleuzen, V. Marvaud, J. Vaissermann, M. Seuleiman, C. Desplanches, A. Scuiler, C. Train, R. Garde, G. Gelly, C. Lomenech, J. Rosenman, P. Veillet, C. Cartier and F. Villain, *Coord. Chem. Rev.*, 1999, **190–192**, 1023; (*d*) J. A. McCleverty and M. D. Ward, *Acc. Chem. Res.*, 1998, **31**, 842; (*e*) S. Decurtins and R. Pellaux, *Comments Inorg. Chem.*, 1998, **20**, 143.

2 (*a*) H. Atzkern, P. Bergerat, M. Beruda, M. Fritz, J. Hiermeier, P. Hudeczek, O. Kahn, F. H. Köhler, M. Paul and B. Weber, *J. Am. Chem. Soc.*, 1995, **117**, 997; (*b*) H. Atzkern, M. Fritz, J. Hiermeier, P. Hudeczek, O. Kahn, B. Kanellakopulos, F. H. Köhler and M. Ruhs, *Chem. Ber.*, 1994, **127**, 277.

3 (*a*) S. Rittinger, D. Buchholz, M. H. Delville-Desbois, J. Linarès, F. Varret, R. Boese, L. Zsolnai, G. Huttner and D. Astruc, *Organometallics*, 1992, **11**, 1454; (*b*) P. Hudeczek and F. H. Köhler, *Organometallics*, 1992, **11**, 1773; (*c*) H. Hilbig, P. Hudeczek, F. H. Köhler, X. Xie, P. Bergerat and O. Kahn, *Inorg. Chem.*, 1998, **37**, 4246; (*d*) M.-H. Delville, F. Robert, P. Gouzerh, J. Linarès, K. Boukheddaden, F. Varret and D. Astruc, *J. Organomet. Chem.*, 1993, **451**, C10; (*e*) P. Hudeczek, F. H. Köhler, P. Bergerat and O. Kahn, *Chem. Eur. J.*, 1999, **5**, 70.

4 J. M. Manriquez, M. D. Ward, W. M. Reiff, J. C. Calabrese, N. L. Jones, P. J. Carrol, E. E. Bunel and J. S. Miller, *J. Am. Chem. Soc.*, 1995, **117**, 6182.

5 (*a*) J. Schweizer and E. Ressouche, in *Magnetism: Molecules to Materials*, ed. J. S. Miller and M. Drillon, Wiley-VCH, New York, p. 325.; (*b*) B. Gillon, in *Magnetism: Molecules to Materials*, ed. J. S. Miller and M. Drillon, Wiley-VCH, New York, p. 357.; (*c*) F. H. Köhler, in *Magnetism: Molecules to Materials*, ed. J. S. Miller and M. Drillon, Wiley-VCH, New York, p. 379.

6 (*a*) G. E. McManis, R. M. Nielson and M. J. Weaver, *Inorg. Chem.*, 1988, **27**, 1827; (*b*) M.-H. Delville, S. Rittinger and D. Astruc, *J. Chem. Soc., Chem. Commun.*, 1992, 519.

7 (*a*) A. Bauer, H. Hilbig, W. Hiller, E. Hinterschwepfinger, F. H. Köhler and M. Neumayer, *Synthesis*, 2001, 778; (*b*) H. Hilbig, F. H. Köhler and K. Mörtl, *J. Organomet. Chem.*, 2001, **627**, 71.

8 E. E. Bunel, L. Valle and J. M. Manriquez, *Organometallics*, 1985, **4**, 1680.

9 P. J. McCarthy and H. K. Güdel, *Coord. Chem. Rev.*, 1988, **88**, 69.

10 D. Buchholz, B. Gloaguen, J. F. Fillaut, M. Cotrait and D. Astruc, *Chem. Eur. J.*, 1995, **1**, 374.

11 F. H. Köhler and K. H. Doll, *Z. Naturforsch. B*, 1982, **37**, 144. Note that the shift sign convention has changed since.

12 (*a*) F. H. Köhler, K.-H. Doll and W. Prössdorf, *Angew. Chem., Int. Ed. Engl.*, 1980, **19**, 476; (*b*) F. H. Köhler and W. A. Geike, *J. Organomet. Chem.*, 1987, **328**, 35.

13 R. H. Weshall and I. Shain, *Anal. Chem.*, 1967, **37**, 1514.

14 Y. F. Oprunenko, *Russ. Chem. Rev.*, 2000, **69**, 683.

15 Y. A. Ustynyuk, O. I. Trifonova, Y. F. Oprunenko, V. I. Mstislavsky and I. P. Gloriozov, *Organometallics*, 1990, **9**, 1707.

16 T. A. Albright, P. Hofmann, R. Hoffmann, C. P. Lillya and P. A. Dobosh, *J. Am. Chem. Soc.*, 1983, **105**, 3396.

17 L. Banci, I. Bertini and C. Lucinat, *Struct. Bonding*, 1990, **72**, 113 and literature cited therein.

18 M. M. Sabbatini, *Inorg. Chim. Acta*, 1977, **24**, L9.

19 F. H. Köhler, B. Metz and W. Strauss, *Inorg. Chem.*, 1995, **34**, 4402.

20 H. O. Kalinowski, S. Berger and S. Braun, *^{13}C-NMR-Spektroskopie*, Georg Thieme Verlag, Stuttgart, 1984, p. 74.

21 R. J. Kurland and R. B. McGarvey, *J. Magn. Reson.*, 1970, **2**, 286.

22 C. Mealli and D. M. Prosperio, *Chem. Educ.*, 1990, **67**, 399.

23 (*a*) G. Rabe, H. W. Roesky, D. Stalke, F. Pauer and G. M. Sheldrick, *J. Orgamnomet. Chem.*, 1991, **403**, 11; (*b*) A. Hammel and W. Schwarz, *Acta Crystallogr., Sect. C*, 1990, **46**, 2337; (*c*) P. Seiler and J. D. Dunitz, *Acta Crystallogr., Sect. B*, 1980, **36**, 2255; (*d*) J. Trotter, *Acta Crystallogr.*, 1961, **14**, 1135.